Improved solution reliability through generalised finite integral methods

A. G. Barnett

ABSTRACT

Model solution reliability is shown to be important for applications, where the computational method should accommodate a wide range of flow conditions through each model run without failure through instability or excessive run times. Such difficulties are linked to the use of poor assumptions in the derivation of models, in particular those neglecting energy solutions and the proper treatment of gradient discontinuities and shocks. Finite integral methods are introduced as a formal extension of longstanding traditional hydraulic analysis, leading through Control Element Lifetime Locus (CELL) Integral analysis to a new set of fundamental balance equations, the Full Hydraulic equations. These are then formulated for hydraulic streamtube analysis and discretised for separate numerical solutions for momentum and energy balances. Case studies for steady flow are referenced, where CELL energy balances improve solution robustness through a variable weighting scheme, accelerating convergence in comparison with widely used fixed weighting Upstream Differencing and Central Differencing schemes. A standard dambreak case study is then used to show the same robust system also copes with severe unsteady flow discontinuities, even while Courant Numbers are varied by orders of magnitude.

Key words | CELL Integrals, convergence, energy balances, streamtubes, variable weighting

A. G. Barnett
HYDRA Software Ltd,
PO Box 9463,
Hamilton 3240,
New Zealand
E-mail: *barncon@xtra.co.nz*

INTRODUCTION

Computational model applications are typically commissioned on the basis that results are to be produced in a limited time, making the best of inadequate available field data observations. In selecting the method of analysis, an applied model user therefore attaches high value to the reliability of the solution, so that the chosen method should not fail through instability or excessive run times, even though field data limitations often impose the concentration of validation data in a few areas. This leaves minimal data in large intervening regions, so ideally the preferred method should offer robust performance throughout a range of widely flexible grid spacing, both timewise and spacewise.

In practice, the first generation of solution methods suffered from problems with instability and inconsistency – see Abbott (1979) – so solution reliability demanded a considerable background in numerical analysis from the model user, with corresponding constraints, particularly the Courant limitation on the explicit time step used. These constraints were eased by the introduction of implicit solution methods which were first thought to be unconditionally stable. However, Barnett (1974) showed that the claimed unconditional stability was valid only for pure initial value problems, as the addition of boundary conditions produced stability limitations related to the Froude Number, applying particularly with Courant Numbers less than unity. Further, in practice, implicit schemes were then found to be unreliable through susceptibility to phase errors (Cunge *et al.* 1980). According to finite difference analysis, second order schemes are theoretically superior to first order schemes, but if shocks developed in the solution, oscillations in the vicinity then appeared with such higher order schemes, tending to corrupt the solution.

doi: 10.2166/hydro.2013.048

Subsequent methods of dealing with such oscillations were discussed by Garcia-Navarro & Burguete (2006), but unfortunately, shock capturing approaches such as the Lax-Wendroff scheme return to an explicit formulation, which reintroduces the unwanted Courant limitation on the time step used. Upwinding schemes are also introduced to the discussion, but generally, attempts to make these implicit seem to have been seen as too difficult for general application. In the discussion, several schemes were compared with an exact analytical solution of a dambreak problem, and the 'excessive numerical diffusion introduced by the first order central scheme and the lack of robustness of the second order scheme are shown'. The writers then comment 'Roe's scheme, being only first order, is very well suited' for this kind of problem.

In short, the authors make clear that second order schemes do not necessarily produce more reliable solutions than first order schemes, contrary to the conclusion suggested by finite difference analysis. Further, use of these more advanced schemes seems in practice to require the sacrifice of relative freedom from time step size restrictions enjoyed by implicit schemes. As noted above, this becomes a major disadvantage in many practical applications of computational solutions.

Guinot (2000) raised another difficulty related to advection modelling in multiple dimensions for strongly divergent flows. Both finite difference and finite volume solutions are considered. A corrective solution is proposed, but again this correction imposes an unwanted limitation on the computational time step.

The methods discussed above are mainly based on an Eulerian view, although Garcia-Navarro & Burguete (2006) also briefly discuss Lagrangian and characteristic views, describing the latter as 'Semi-Lagrangian' because although they are based on an Eulerian grid they carry directional information. However, the characteristic solution grid is based on wave speeds rather than particle velocities as in true Lagrangian solutions.

Finite integral balances in hydraulics

To avoid premature choices restricting the algorithmic options available for computational solution, it is valuable to derive balance equations expressing conservation laws of energy, momentum and mass without restriction to an Eulerian or Lagrangian or characteristic view.

Hydraulic engineering texts routinely do this informally: for example, with reference to the storage of water in a river reach. Over a finite time interval, the volume balance (or mass balance if density is constant) can be expressed (e.g., Henderson 1966) as

Inflow volume − outflow volume = increase in storage

This is true whether the 'inflow volume' and 'outflow volume' refer to cross-sections which are fixed (Eulerian), moving at flow velocity (Lagrangian), or at the speed of a surge discontinuity (characteristic). The 'storage' generally refers to the volume bounded by the two cross-sections at the ends, by the river bed below and laterally, and by the free surface above. If the river bed is fixed, the Eulerian view applies, but the free surface takes the same character as the cross-sections horizontally while matching the surface velocity vertically. This means that, depending on the definition of the end sections, it is some mixture of Eulerian, Lagrangian and characteristic.

This combination of a semi-Lagrangian free surface with an Eulerian boundary for the ends and channel bed to define the control element for conservation laws is generally attributed to St Venant (Cunge *et al.* 1980), so could be described as 'St Venantian'. Note that in steady flow this approach is comparable with the finite volume technique, in the sense that treatment of one dimension (in this case, the longitudinal channel coordinate) as an analytic continuum is combined with discrete treatment of finite integrated cross-section elements in the remaining spatial dimensions. In unsteady flow, as with finite volume techniques, treatment of the time dimension as a second continuum again introduces analytical problems in cases where discontinuities propagate along characteristics. However, because of the popularity of this approach in shallow water modelling, it is important to generalise any fundamental expressions to incorporate the St Venantian control element as well as the more traditional Eulerian and Lagrangian viewpoints.

Generalised control element balances

In order to set up balance equations for a *region of space R*, a *control surface A* must be defined with respect to a *reference frame*. Without these conceptual constructions, distributions of properties such as mass, momentum and energy cannot be discussed in any satisfactory quantitative manner. Here we take as a reference frame an inertial frame which has the property of moving at an arbitrary constant velocity $\boldsymbol{U}$ relative to some base reference frame, which is also inertial. The relativity principle (Landau & Lifshitz 1972) states that all the laws of nature are the same to an observer moving at any constant velocity, so conservation laws must apply equally in both reference frames. Figure 1 illustrates these concepts.

Control Element Lifetime Locus (CELL)

The control surface is spatially closed to separate an 'inside' from an 'outside', meaning that any selected mass particle can move between the inside and the outside *only* by passing through that surface. Therefore as well as the change in status from counting (inside) to not counting (outside), this change can also be accounted for as a spacewise flux. Further, taking a relativistic viewpoint (Barnett 1994) to extend closure into four dimensions, the control surface exists only for a finite lifetime from time $t = t_1$ to $t = t_2$, so that 'before' and 'after' closure both count as outside that surface while 'during' closure counts as inside. This means the particle can also move between inside and outside simply by being within the spatial surface at the beginning or end of its lifetime, effectively adding a timewise flux component.

Finally, the control surface in general moves at some velocity $\boldsymbol{u}$ varying from point to point and time to time, so that the element contained within the surface follows some locus, possibly varying in shape during its lifetime. The whole construction is therefore conveniently described by the acronym CELL.

For the CELL pictured in Figure 1, the energy balance equation is

$$\left[\int_R \left(\frac{v^2}{2}+e\right)\rho dR\right]_{t_1}^{t_2} + \int_{t_1}^{t_2}\int_A \boldsymbol{n}.(\boldsymbol{v}-\boldsymbol{u})\left(\frac{v^2}{2}+e\right)\rho\, dA\, Dt = \int_{t_1}^{t_2}\int_R \boldsymbol{f}.\boldsymbol{v}\rho\, dR\, Dt + \int_{t_1}^{t_2}\int_A \boldsymbol{n}.\boldsymbol{\sigma}.\boldsymbol{v}\, dA\, Dt - \int_{t_1}^{t_2}\int_A \boldsymbol{n}.\boldsymbol{q} dA\, Dt \tag{1}$$

where the physical parameters follow common terminology: $\boldsymbol{v}$ is the fluid velocity in the inertial frame, e is the internal energy per unit mass, ρ is the mass density, dR is an element of the countable volume inside the surface, $\boldsymbol{n}$ is the normal to the surface (positive outwards), dA is an element of the area of the surface, Dt is a time increment, written with a capital D as it is 'following the element' during its existence between t_1 and t_2, $\boldsymbol{f}$ is the body force per unit mass, $\boldsymbol{\sigma}$ is the stress tensor at the surface and $\boldsymbol{q}$ is the heat flux density.

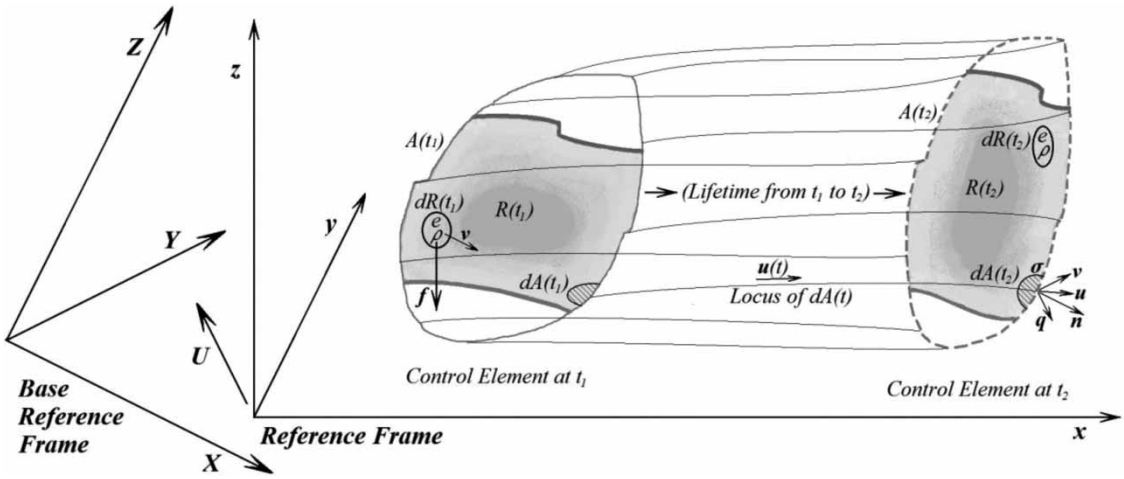

Figure 1 | Definition of a CELL (Control Element Lifetime Locus).

This is the energy balance in the ordinary reference frame. Transforming into the base reference frame

$$\left[\int_R \left(\frac{(\boldsymbol{v}+\boldsymbol{U})\cdot(\boldsymbol{v}+\boldsymbol{U})}{2}+e\right)\rho dR\right]_{t_1}^{t_2} + \int_{t_1}^{t_2}\int_A \boldsymbol{n}.(\boldsymbol{v}+\boldsymbol{U}-(\boldsymbol{u}+\boldsymbol{U}))\left(\frac{(\boldsymbol{v}+\boldsymbol{U})\cdot(\boldsymbol{v}+\boldsymbol{U})}{2}+e\right)\rho dA\,Dt = \int_{t_1}^{t_2}\int_R \boldsymbol{f}.(\boldsymbol{v}+\boldsymbol{U})\rho\,dR\,Dt + \int_{t_1}^{t_2}\int_A \boldsymbol{n}.\boldsymbol{\sigma}.(\boldsymbol{v}+\boldsymbol{U})\,dA\,Dt - \int_{t_1}^{t_2}\int_A \boldsymbol{n}.\boldsymbol{q}dA\,Dt \quad (2)$$

On the basis that $\boldsymbol{U}$ is a constant vector, this can be rearranged into the form

$$E + \boldsymbol{U}.\boldsymbol{M} + \frac{1}{2}U^2 I = 0 \quad (3)$$

where E is defined by

$$E = \left[\int_R \left(\frac{\boldsymbol{v}^2}{2}+e\right)\rho dR\right]_{t_1}^{t_2} + \int_{t_1}^{t_2}\int_A \boldsymbol{n}.(\boldsymbol{v}-\boldsymbol{u})\left(\frac{\boldsymbol{v}^2}{2}+e\right)\rho\,dA\,Dt - \int_{t_1}^{t_2}\int_R \boldsymbol{f}.\boldsymbol{v}\rho\,dR\,Dt + \int_{t_1}^{t_2}\int_A \boldsymbol{n}.\boldsymbol{\sigma}.\boldsymbol{v}\,dA\,Dt - \int_{t_1}^{t_2}\int_A \boldsymbol{n}.\boldsymbol{q}dA\,Dt \quad (4)$$

The vector $\boldsymbol{M}$ is defined by

$$\boldsymbol{M} = \left[\int_R \boldsymbol{v}\rho dR\right]_{t_1}^{t_2} + \int_{t_1}^{t_2}\int_A (\boldsymbol{n}.(\boldsymbol{v}-\boldsymbol{u}))\boldsymbol{v}\rho\,dA\,Dt - \int_{t_1}^{t_2}\int_R \boldsymbol{f}\rho\,dR\,Dt + \int_{t_1}^{t_2}\int_A \boldsymbol{n}.\boldsymbol{\sigma}dA\,Dt \quad (5)$$

and I is defined by

$$I = \left[\int_R \rho\,dR\right]_{t_1}^{t_2} + \int_{t_1}^{t_2}\int_A \boldsymbol{n}.(\boldsymbol{v}-\boldsymbol{u})\rho\,dA\,Dt \quad (6)$$

If Equation (3) is to be satisfied for any arbitrary $\boldsymbol{U}$, $\boldsymbol{M}$ must be a null vector, i.e., $\boldsymbol{M}=\boldsymbol{0}$, and the scalars E and I must both be zero. $E=0$ is simply a restatement of the scalar Equation (1), while the vector equation $\boldsymbol{M}=\boldsymbol{0}$ requires that

$$\left[\int_R \boldsymbol{v}\rho\,dR\right]_{t_1}^{t_2} + \int_{t_1}^{t_2}\int_A (\boldsymbol{n}.(\boldsymbol{v}-\boldsymbol{u}))\boldsymbol{v}\rho\,dA\,Dt = \int_{t_1}^{t_2}\int_R \boldsymbol{f}\boldsymbol{\rho}\,dR\,Dt + \int_{t_1}^{t_2}\int_A \boldsymbol{n}.\boldsymbol{\sigma}\,dA\,Dt \quad (7)$$

The scalar equation $I=0$ requires that

$$\left[\int_R \rho\,dR\right]_{t_1}^{t_2} + \int_{t_1}^{t_2}\int_A \boldsymbol{n}.(\boldsymbol{v}-\boldsymbol{u})\rho\,dA\,Dt = 0 \quad (8)$$

Equation (7) can be seen as a vector statement of the CELL conservation of momentum, while Equation (8) is the CELL conservation of mass statement. The mass balance is the simplest form of conservation law, in which the first term represents the timewise flux balance, or change in mass countable inside the surface, while the second term represents the spacewise flux balance, which accounts for the mass passing through the surface. The plus sign derives simply from the choice of convention that the normal vector $\boldsymbol{n}$ is positive outwards, so that outflows are counted as positive.

Since there are no source terms, so that all the terms are fluxes through either a spatial or timewise boundary, Equation (8) could be recast purely as a four-dimensional surface integral. However, this does not apply to the more complicated Equations (1) and (7), which include source terms, so any added elegance of presentation is unlikely to contribute to practical solutions of the balance equations.

The Full Hydraulic equations

Classical hydraulics has always used both energy and momentum principles, with particular emphasis on Bernoulli analysis, which derives from the energy principle provided that the body force per unit mass $\boldsymbol{f}$ acts through a conservative gravitational field, so that $\boldsymbol{f}=\boldsymbol{g}$, the acceleration of gravity. Standard textbooks such as Henderson (1966) placed great emphasis on teaching the distinction between energy and momentum equations for association with the mass conservation equation in successful steady flow analysis. Although unsteady equation systems are commonly regarded as a generalisation of steady equation systems, they cannot be used for steady hydraulic analysis if they do not reduce in the steady limit to the classical distinct energy, momentum and mass equations.

To provide the same flexibility as in classical hydraulics, the analyst must not be bound in advance to a global choice of energy or momentum analysis. The momentum Equation (5) requires evaluation of the surface stress tensor $\boldsymbol{\sigma}$ over the

entire boundary of the control element, a challenging task in irregular channels of varying cross-section. In contrast, where flow can be visualised in terms of streamlines and streamtubes, energy analysis has the great advantage of eliminating all normal effects of the surface stress tensor along the sides of the control element simply by defining this as a streamtube, because the external work done by normal stresses is then zero. This is an alternative view of the simplification offered by the Bernoulli equation, which was derived before the invention of thermodynamics. If the streamtube is taken as the whole channel, then use of a no-slip condition requires that the velocity is zero at all points along the sides of the control element. In this case, shear forces also do no work, so the entire stress tensor can be eliminated from all but end boundaries of the control element.

Such cases are common in hydraulics, which is essentially concerned with flow in channels, so the energy equation is more generally applicable in hydraulic analysis, particularly through structures such as natural or artificial weirs. However, if a hydraulic jump or pressure shock is discovered to develop during the solution, momentum analysis is a more accurate choice in the vicinity. CELL integrals support this flexibility, as momentum-based and energy-based CELLs may be placed directly adjacent to each other timewise or spacewise without affecting the integrity of the internal balance equations. However, as with any adjacent CELLs, the interfaces between must be defined to move in a mutually compatible way.

The classic St Venant equations (for example, see Cunge *et al.* 1980) deal only with momentum and mass. Therefore they do not reduce to distinct energy, momentum and mass forms in the steady limit, so are unusable for complete steady hydraulic analysis. It follows that they are also unsuitable for generalised unsteady hydraulic analysis.

Equation (3) was first developed by Barnett (1994, 1995), encapsulating five independent equations – the scalar energy and mass balances and the three components of the vector momentum equation. These equations have the required properties in the steady limit, so are called the 'Full Hydraulic' equations.

Note that the basis of the three vector components has yet to be defined. The use of $\boldsymbol{x}$, $\boldsymbol{y}$ and $\boldsymbol{z}$ to label the axes of the reference frame is normally associated with Cartesian coordinates, but no use has been made of that convention to this point, as the algebra of vectors and tensors can be applied without direct reference to axes (for example, see Milne-Thomson 1972). Although Cartesian axes are widely used, other systems of coordinates such as spherical polar coordinates or cylindrical coordinates are also convenient in hydrodynamics, and Figure 1 does not exclude these interpretations of $\boldsymbol{x}$, $\boldsymbol{y}$ and $\boldsymbol{z}$. In particular, streamtubes are most easily analysed using quasi-cylindrical coordinates, based on the curvilinear axis of the tube plus two orthogonal coordinates covering the cross-sections.

Incorporation of existing classical formulations

The control surface velocity $\boldsymbol{u}$ is a conceptual aid rather than a physical property, and is therefore entirely under the control of the analyst. For example, the Full Hydraulic equations can be recast in Eulerian form simply by applying the vector setting $\boldsymbol{u} = \boldsymbol{0}$ throughout the CELL.

Similarly, the Lagrangian view can be recovered by applying the vector setting $\boldsymbol{u} = \boldsymbol{v}$ at all control surfaces. Wave motions such as dynamic and kinematic waves, as well as shocks such as water hammer pulses, all have characteristic wave speeds (Henderson 1966) which can be referred to in general as a 'celerity' $\boldsymbol{c}$. The device of simplifying analysis by adopting the viewpoint of an observer moving along the wave or shock characteristic is therefore equivalent to setting $\boldsymbol{u} = \boldsymbol{c}$ at all control surfaces, producing the Full Hydraulic equations in characteristic form. (This is strictly true only where a single characteristic celerity dominates, as with strong shocks or kinematic wave solutions. Where multiple characteristics are important, manipulation of combinations of the equations is required to produce a characteristic form.)

Finally, the St Venantian view can be recovered by applying the Eulerian setting $\boldsymbol{u} = \boldsymbol{0}$ to all control surfaces except the free surface, where the kinematical condition $(\boldsymbol{v} - \boldsymbol{u}).\boldsymbol{n} = 0$ (Milne-Thomson 1972) should be applied. This can be interpreted as $\boldsymbol{u}$ being a vector normal to the free surface at any instant, with the same magnitude as the normal component of $\boldsymbol{v}$ at the same instant.

Differential formulation

Conservation laws are often refined to a differential form. For example, the mass balance in the form found in texts

such as Batchelor (1970) is reached by assuming an Eulerian frame, so the surface is fixed with respect to the observer, and $\boldsymbol{u} = 0$.

Additional assumptions are also required:

(i) All variables are analytic with respect to time, so that first timewise differentials exist.

Then, Equation (8) can be rewritten as

$$\int \left\{ \frac{\partial \rho}{\partial t} + \nabla.(\rho \boldsymbol{v}) \right\} dV = 0$$

and hence, if the integrand is continuous

$$\frac{\partial \rho}{\partial t} + \nabla.(\rho \boldsymbol{v}) = 0$$

However, Batchelor does note that discontinuities may appear in the solution at various 'points, lines or surfaces', in which case the differential form 'holds everywhere except possibly at these points, lines or surfaces'. This assumption of continuity may be written as:

(ii) The terms on the left-hand side of the differential equation are a continuous function of position.

For this reason, this differential equation is often called the 'equation of continuity'. It also provides the mass balance part of the Navier–Stokes equations, which are often regarded as fundamental.

Unfortunately, in hyperbolic problems which are the basis of wave mechanics, neither assumptions (i) nor (ii) are in general true, as it is well known (Cunge *et al.* 1980) that disturbances propagate along characteristic lines, and these typically involve gradient discontinuities. In more severe cases, shocks develop which introduce discontinuities in the basic fluid properties, so that within the shock zones the differential coefficients do not even exist.

In case anyone believes that such shock zones can ultimately be resolved by adopting a sufficiently high resolution for analysis, Landau & Lifshitz (1959) estimate that the thickness of a strong shock is of the same order as the mean free path of the fluid molecules. In macroscopic fluid dynamics, the fluid is treated as a continuous medium, so they conclude 'the mean free path must be taken as zero'. Also, the use of an Eulerian frame introduces a discontinuity at the free surface in unsteady problems, because the free surface is again generally considered to be only a few molecules thick.

In short, although the Navier–Stokes equations can be derived from the Full Hydraulic equations, additional restrictive assumptions are required, and the energy equation is discarded, so the Full Hydraulic equations cannot be recovered from the Navier–Stokes equations. Therefore for computational purposes, the Navier–Stokes differential equations are a less fundamental starting point than the Full Hydraulic integral equations.

Abbott (1979) identifies the problem as 'an opposing of the discrete view of processes to the more familiar continuum view'. Since a whole generation has passed since this fundamental work was published without any evident reduction in reliance on the convenience of differential notation, the present paper proposes a modified notation which makes explicit the restriction to zones of continuity.

Use of the mathematical 'ni' symbol ∋ seems appropriate for such restriction, as the usual definition (W3C Working Draft 2012) is 'contains as member' or 'reverse element, such that'. For example, $\partial \rho_{\ni} / \partial t$ would then mean 'the partial differential of ρ (but only in the subset of places where this varies continuously) with respect to t'. This would refer to assumption (i), and corresponding references could be made to spatial derivatives with respect to assumption (ii). In most cases, spacewise discontinuities imply timewise discontinuities, as wave disturbance characteristics propagate in both space and time, so in general there is no good reason to adopt timewise continuity (assumption (i)) without also adopting spacewise continuity (assumption (ii)).

Finite difference expressions

According to standard finite difference procedures, the value of $\rho(t_2)$ can be expressed as a Taylor Series:

$$\rho(t_2) = \rho(t_1) + \frac{\partial \rho_{\ni}}{\partial t}(t_1)(t_2 - t_1) + \frac{\partial^2 \rho_{\ni}}{\partial t^2}(t_1)\frac{(t_2 - t_1)^2}{2!} + \ldots$$

Truncation to the first term of this Taylor Series expansion gives a first order approximation, truncation to the second term gives a second order approximation, and so

on. In the subset of places where ρ and its higher derivatives vary continuously, the second order approximation should be more accurate than the first order approximation according to longstanding textbook arguments based on Maclaurin's expansion. However, if assumption (i) is discarded, this does not affect the status of the first term in Equations (1), (7) and (8) as a definite integral, which can be interpreted as an exact first difference!

In this more general case, any attempt to add higher order terms will therefore simply introduce corresponding error terms. This is the reverse of the situation with finite difference analysis, in which the inclusion of such terms is viewed as *removing* errors of the same order! This suggests a reason why first differences are found empirically to be superior to higher order differences in cases such as those discussed by Garcia-Navarro & Burguete (2006), even though Taylor Series analysis suggests the opposite should be true.

Note first order accuracy applies only to the *differencing* of the fluxes through the boundary surface – the computational *integration* of these fluxes over the continuous region R at times t_1 and t_2 in Equations (1), (7) and (8) is still a matter for numerical quadrature, and this may well benefit from the introduction of higher order interpolating functions.

These same arguments extend to the second term in Equations (1), (7) and (8), but with temporal and spatial components exchanged. With careful distinction between surface integrals which form exact first differences, and volume integrals which deal with continuously existing distributions, the Full Hydraulic equations provide a sound basis for solution schemes which improve on the accuracy of all finite difference solutions, especially in the presence of weak and strong shocks. The test for this is improvements in the reliability of solutions, the subject of this paper.

Shock capturing schemes

Shock capturing schemes which apply integral balances across shocks have been well known since the Lax-Wendroff scheme mentioned earlier. The theory of weak solutions was well discussed by Abbott (1979). However, this theory has since been treated as applicable only where discontinuities occur as shocks, whereas in fact integral balances apply equally to continuous flow. In particular, gradient discontinuities pervade any solution where these are introduced as boundary conditions, for example through the common practice of representing a boundary flow or level by a segmented time series. In such cases, the use of Taylor Series for finite difference analysis is non-rigorous.

Therefore shock capturing schemes may have reliability comparable with CELL Integral methods, but only if integral balances are used consistently in all parts of the solution, and not substituted by finite difference methods where shocks are not prominent. The Lax-Wendroff scheme, for example, is less reliable because the explicit stability condition introduces strict stability limits which cannot be avoided with confidence when the solution (including applicable celerities) is not yet available.

Finite volume methods

These methods are similar to CELL Integrals in the aim of improving the treatment of shock discontinuities, and assumption (ii) is avoided by the use of spatial integration. However the relativistic symmetry between space and time is ignored in these procedures, so that assumption (i) is still invoked and finite differences are introduced for time variations – see Garcia-Navarro & Brufau (2006), Guinot (2000) or Norris *et al.* (2011). Further, most applications of finite volumes appear to discard the energy equation without discussion, treating only momentum and mass balances.

Therefore finite volumes have limited value in developing reliable computational wave mechanics, as they are a restricted subset of the more general CELL Integrals. The two methods overlap only where the energy equation is not computationally attractive, and where the problem can be reduced to a steady state by suitable manipulation of the locus of the finite volume. Within this subset of problems the effects of assumption (i) are negligible, so the two methods can then be expected to produce virtually identical results.

Reliability and robustness

'Reliability' is a rather subjective term, but an objective measure of reliability can be developed by introducing

solution 'robustness', defined as the assessable property of continuing to provide a fair approximation to a solution even if grid spacing and Courant Numbers are allowed to vary by orders of magnitude. Barnett (2012) linked solution robustness to the *rate* of convergence of a scheme, which was shown to vary greatly between alternative widely used schemes.

Admittedly a 'fair approximation' still has a subjective element based on the judgement of the analyst, but at least it absolutely excludes solutions which fail to run to completion through termination by instability. If a solution is obtained, then assessment of a 'fair approximation' should also take into account model uncertainty, of which a good overview is provided by Samuels (2006).

This is of great importance, as the validity of computational solution techniques is often demonstrated under ideal academic conditions: fine grid discretisation at equally spaced steps. In physically based applied models the reality is different, as applied users attach high value to reduction of solution time, and flexibility in grid spacing. Under these conditions, some solutions are robust, performing with minimal loss of accuracy compared with ideal conditions, while others will collapse and report solution failure.

Convergence is the ability of a solution to reach and maintain a final value under successive grid refinements, and widely accepted theory states that all schemes have this property subject to requirements of stability and consistency. This implies that all convergent schemes should ultimately produce the same solution. However, robust schemes will approach this ultimate solution at grid spacings much coarser than those of other schemes.

FORMULATION: HYDRAULIC ANALYSIS

The St Venantian approach is based on streamtube elements in which all flow is nearly parallel with the streamtube axis. Over any cross-section, flow at any point can be resolved into an exactly parallel primary flow component and a transverse secondary flow component. Provided primary flows are dominant, analysis assuming parallel flow establishes that conditions are hydrostatic transverse to the streamtube, so that with constant density the water level is horizontal across each section.

'One-dimensional' analysis

Recently, such streamtube-based analysis has popularly been termed 'one-dimensional', a misleading description as the basic streamtube is fully three-dimensional. For example, if projected onto a horizontal surface, a map of the streamtube appears which is fully two-dimensional. Projections of cross-sections are also two-dimensional, as can be seen from any textbook on hydraulics.

It seems the term 'one-dimensional' has arisen only since the extension of two-dimensional modelling from coastal waters to overland flows. Clearly, streamtube-based modelling is not two-dimensional, so by default it is supposed to be one-dimensional. This may be a reasonable description of a two-dimensional model in which one dimension is suppressed, but such a model is an extreme simplification of a streamtube-based model, requiring among other things restriction to momentum analysis along a prismatic channel of wide rectangular cross-section.

In contrast, the St Venantian approach treats transverse dimensions by integration and the longitudinal dimension by analysis. Certainly this approach is anisotropic, but this does not mean that variation over the transverse dimensions is neglected. On the contrary, use is here being made of 'no-slip' boundary velocity conditions to eliminate the work done by both normal and shear stresses along the bed and walls of the channel streamtube. Also the 'one-dimensional' tag discounts much classical work on parallel flow profiles, such as that by Prandtl on boundary layers (see Henderson 1966).

Since streamtube analysis has such a strong history in classical hydraulics, from Bernoulli to St Venant to Prandtl, it is suggested that where it is to be contrasted with two-dimensional hydrodynamic analysis, the term 'hydraulic analysis' would be far more accurate than 'one-dimensional analysis'.

Dependent variables

Two dependent variables may be selected for solution. The pair flow Q and mean surface water level h are preferred

here, because both have a single value across a cross-section. In contrast, other choices such as depth or depth-averaged velocity measurably vary significantly across typical channels, creating significant unnecessary complications with the linearisation required for analysis. Also, in most circumstances, Q and h vary only gradually along a streamtube. The relative simplicity of the Q, h pair is illustrated by the expression of the hydrostatic solution for all parts of a network as the elementary $Q = 0$, $h = constant$. Since this is also the exact hydrodynamic solution in such conditions, it is easy to use a static solution to initiate computation even for complex model networks.

Integral balances

Cunge *et al*. (1980) show how, for a streamtube-based control element, the integral mass balance (Equation (8)) may be rewritten:

$$\int_{x_1}^{x_2} [(A)_{t_2} - (A)_{t_1}]dx + \int_{t_1}^{t_2} [(Q)_{x_2} - (Q)_{x_1}]dt = 0 \tag{9}$$

Here, x is the distance along the streamtube axis. $A(x, t)$ is the cross-section area and $Q(x, t)$ is the flow (or discharge) variable introduced above.

Since the time differencing of A takes place without variation in x at each cross-section, familiar partial differentials may be introduced to replace $[(A)_{t_2} - (A)_{t_1}]$ by

$$\int_{t_1}^{t_2} (\partial A/\partial t)dt$$

A similar argument for the differencing of Q means the mass balance Equation (8) may be written

$$\int_{x_1}^{x_2}\int_{t_1}^{t_2} \left[\frac{\partial A}{\partial t} + \frac{\partial Q}{\partial x}\right] dt\,dx = 0 \tag{10}$$

If this is left as a double integral, no assumption is required that $\partial A/\partial t$ is continuous, or even exists at all points, as integration to produce $[(A)_{t_2} - (A)_{t_1}]$ is possible even if A exhibits strong discontinuities such as step functions.

The corresponding formulation of Equation (7) for momentum is (cf. Cunge *et al*. 1980)

$$\int_{x_1}^{x_2}\int_{t_1}^{t_2} \left[\frac{\partial Q}{\partial t} + \frac{\partial}{\partial x}\left(\frac{Q^2}{A}\right) + gA\frac{\partial h}{dx} + gAS_f\right] dt\,dx = 0 \tag{11}$$

Here, $h(x, t)$ is the level variable introduced above (called y by Cunge *et al*. 1980), g is the acceleration of gravity and S_f is the 'friction slope' which accounts for shear stresses in Equation (7).

The corresponding formulation of Equation (1) for energy is

$$\int_{x_1}^{x_2}\int_{t_1}^{t_2} \left[\frac{\partial}{\partial t}\left(\frac{Q}{A}\right) + \frac{\partial}{\partial x}\left(\frac{Q^2}{2A^2} + gh\right) + gS_e\right] dt\,dx = 0 \tag{12}$$

Here, S_e is the 'energy slope' which accounts for internal energy and heat fluxes in Equation (1). As can be seen from the dimensions of Equation (12), use has been made of division by the mean of the end flows to produce the energy equation in Bernoulli form. An equivalent manipulation of the differential equations is presented by Abbott (1979).

In steady uniform flow, all variables are continuous and Q and A are both constant, so Equation (11) becomes $S_f = -\partial h/\partial x$ and Equation (12) becomes $S_e = -\partial h/\partial x$. This means under such conditions there is an algebraic equality between S_f and S_e even though one represents wall shear forces and the other incorporates changes in internal energy when wall shear forces do no work.

Since the Manning formula for resistance to flow locally assumes steady uniform flow, both S_f and S_e can be computed using the Manning formula in such conditions. This is

$$S = \frac{Q|Q|n^2P^{4/3}}{M^2A^{10/3}} \text{ where } S \text{ is either } S_f \text{ or } S_e$$

Here, n is the Manning n, P is the wetted perimeter and M is a dimensioned constant $= 1.00\ \mathrm{m}^{1/3}\,\mathrm{s}^{-1}$.

When the cross-section is changing longitudinally, the fundamental difference between the physical basis of friction slope and energy slope becomes important. Energy balances are less affected by expansions and contractions

since wall stresses are no longer relevant, and there are well-established empirical procedures for making allowance for extra factors contributing to the integrated energy slope. For example, at a weir, discharge coefficients have been calibrated to allow for the difference between sharp-edged and square-edged apertures. In contrast, for the momentum balance at a weir, force balances must be based on the aperture dimensions alone without regard for the sharpness of the aperture perimeter, as no comparable laboratory-based body of knowledge is available to discriminate between sharp-edged and square-edged apertures. This is partly because the term $gA(\partial h/\partial x)$ is not in divergent form, so integration with respect to x does not produce a simple first difference.

However, significant generation of internal energy through a hydraulic jump is not easy to measure. The long-accepted method of estimating this has been through the application of momentum balances, as wall stresses often play a comparatively minor role through a jump, so accurate evaluation of the friction slope is far less of a problem than with other changes of cross-section. Once the flow solution is obtained by momentum balances, it can be applied to determine the change in macroscopic energy through the jump, and hence the balancing change in integrated energy slope.

In summary, uniform flow produces solutions which are the same for both momentum and energy balances, so in these circumstances the two methods are practically equivalent even though physically they represent completely different conceptual approaches. However, longitudinal changes in cross-section (either imposed by the channel boundaries or by hydraulic jumps) produce divergence between the two solutions increasing with the severity of the expansion or contraction.

As well explained by classic texts such as Henderson (1966), energy balances are more accessible in the common situations where cross-section changes are imposed by the channel walls and bed, with momentum balances being preferred only for hydraulic jumps. Accordingly, the default CELL Integral method relies on the mass–energy couple. Only if a hydraulic jump develops in this mass–energy solution need transfer be made locally to the mass–momentum couple to refine the solution in the CELLs affected by the jump.

DISCRETISATION

The mass balance Equation (10) is still not in a form suitable for numerical solution. Since quadrature is to proceed in the rectangular space–time element between x_1 and x_2 and t_1 and t_2, the conventional Preissmann four-point scheme is applied. This is described in Cunge *et al.* (1980). In the Preissmann scheme the variables are solved at (x_1, t_2) and (x_2, t_2), and a more compact notation rewrites $Q(x_1, t_2)$ as Q'_u where the dash denotes time t_2 and the subscript u (for upstream) denotes x_1 (or x_u). Correspondingly, h'_d represents $h(x_d, t_2)$ downstream, and so on for h'_u and Q'_d.

For example, the first term in Equation (12) then becomes

$$\int_{x_u}^{x_d} \frac{Q'}{A'} - \frac{Q}{A} dx$$

and this can be linearised for matrix solution by introducing the variation quantities $\dot{Q}_u = Q'_u - Q_u$ and so on. Then

$$\frac{Q'}{A'} = \frac{Q\left(1 + (\dot{Q}/Q)\right)}{A\left(1 + (\dot{A}/A)\right)} \approx \frac{Q\left(1 + (\dot{Q}/Q)\right)\left(1 - (\dot{A}/A)\right)}{A}$$
$$= \frac{Q}{A} + \frac{\dot{Q}}{A} - \frac{Q}{A}\frac{\dot{A}}{A}$$

Here the ratios $\dot{Q}/Q$ and $\dot{A}/A$ are both assumed to be small compared with unity to justify retaining only the linear terms in the series. Further, $\dot{A} \approx B\dot{h}$ where B is the surface width at time t_1, and is therefore available as a known input to the computation. Note linearising has been required only in the timewise sense, as variation spacewise is then governed by the available solution at the previous time step. Therefore no restriction applies to equivalent spacewise ratios, for example $(A_d - A_u)/A_d$. This is important, as such ratios may be very large in a typical natural channel, for example at the exit from a lake into a river.

If (Q/A) is assumed to vary linearly with x, then

$$\int_{x_u}^{x_d} \frac{Q'}{A'} - \frac{Q}{A} dx \approx \left[\frac{1}{A_u}\dot{Q}_u - \frac{Q_u B_u}{A_u^2}\dot{h}_u + \frac{1}{A_d}\dot{Q}_d - \frac{Q_d B_d}{A_d^2}\dot{h}_d\right]\frac{\Delta x}{2} \quad (13)$$

where $\Delta x = x_d - x_u$

More generally, $\int_{x_u}^{x_d} f\,dx = (w_u f_u + w_d f_d)\Delta x$

with w_u and w_d upstream and downstream weights, where usually $w_u + w_d \approx 1$.

With linear variation (or a step function positioned at $x_u + (\Delta x/2)$), $w_u = w_d = 1/2$ as in Equation (13) above. This is strictly the basis of the Preissmann scheme, but often more information is available as the basis of some modified weighting. For example, evaluation of the first term in Equation (9) gives

$$\int_{x_u}^{x_d} A' - A\,dx \approx \int_{x_u}^{x_d} B\dot{h}\,dx$$

When interpolating cross-sections, as well as a linear variation in $\dot{h}$, it is conventional to assume a linear variation in B. This gives a quadratic variation in the product $B\dot{h}$, so as a result

$$\int_{x_u}^{x_d} A' - A\,dx \approx \left(\frac{B_u}{3} + \frac{B_d}{6}\right)\Delta x\dot{h}_u + \left(\frac{B_u}{6} + \frac{B_d}{3}\right)\Delta x\,\dot{h}_d$$

The second term in Equation (9) is treated as described in Cunge *et al.* (1980), so that

$$\int_{t_1}^{t_2} Q(t)dt \approx [\theta Q' + (1-\theta)Q]\Delta t \quad \text{where } \Delta t = t_2 - t_1$$

If the solution is linear, the weighting parameter θ is 1/2, but protection of the solution against instability has been found to require an increase in θ, presumably reflecting occasions where the timewise variation is of higher order such as in the quadratic variation discussed above. Since advance information about the timewise variation of solutions is rarely available in practice, placing the timewise weighting coefficient under the direct control of the model user has been a comparatively successful strategy. CELL Integral analysis follows conventional practice in this respect.

Therefore $\int_{t_1}^{t_2} Q_d - Q_u dt \approx [Q_d - Q_u + \theta\dot{Q}_d - \theta\dot{Q}_u]\,\Delta t$

Summarising, the mass balance equation is formulated for computation as

$$-\theta\Delta t\,\dot{Q}_u + \left(\frac{B_u}{3} + \frac{B_d}{6}\right)\Delta x\,\dot{h}_u + \theta\Delta t\,\dot{Q}_d + \left(\frac{B_u}{6} + \frac{B_d}{3}\right)\Delta x\,\dot{h}_d = (Q_u - Q_d)\Delta t \tag{14}$$

Apart from the example above of the formulation of the first term in Equation (12), space here does not permit presentation of the full derivation of the discretised momentum and energy balances by series expansion from Equations (11) and (12), respectively. Both results can be written as

$$M_{a1}\dot{Q}_u + B_u M_{a2}\dot{h}_u + M_{a3}\dot{Q}_d + B_d M_{a4}\dot{h}_d = M_{a5} \tag{15}$$

Note however that each of the matrix coefficients M_{a1}, M_{a2}, M_{a3}, M_{a4} and M_{a5} differs between the momentum and energy approaches.

Application of the methods described above produces the following coefficients for straightforward parallel flow problems (those excluding lateral flows, shock losses, compound channels, discharge coefficients and steep slopes). The momentum balance uses three auxiliary variables:

$$I_m = \frac{Q_u}{A_u} - \frac{g\,S_{fu}\,A_u w_u\,\Delta x}{Q_u} \quad J_m = \frac{Q_d}{A_d} + \frac{g\,S_{fd}A_d\,w_d\,\Delta x}{Q_d}$$
$$K_m = \frac{g}{2}(A_u + A_d)$$

Note that w_u and w_d are here the weights allocated to the upstream and downstream contributions to S_f (or to S_e for energy), based on the shape of the spacewise solution supplied from the previous time step. Unlike with finite differences, these shapes are not restricted to polynomials. For a backwater profile (detected by $S_u > S_d$) the form is exponential (see Barnett & MacMurray (1998)), while for a drawdown ($S_u < S_d$) the form is an inverse parabola (see Barnett (2012). Then, for momentum

$$M_{a1} = \frac{\Delta x}{2\theta\,\Delta t} - 2I_m$$

$$M_{a2} = -\frac{K_m}{B_u} - \frac{Q_u}{A_u}\left(\frac{Q_u}{A_u} - 2I_m\right) - \frac{g}{2}(h_u - h_d)$$

$$M_{a3} = \frac{\Delta x}{2\theta\,\Delta t} + 2J_m$$

$$M_{a4} = \frac{K_m}{B_d} + \frac{Q_d}{A_d}\left(\frac{Q_d}{A_d} - 2J_m\right) - \frac{g}{2}(h_u - h_d)$$

$$M_{a5} = \frac{1}{\theta}[I_m Q_u - J_m Q_d + K_m(h_u - h_d)]$$

For energy, the auxiliary variables are slightly different:

$$I_e = I_m - \frac{Q_u}{2A_u} \quad J_e = J_m - \frac{Q_d}{2A_d}$$

Then

$$M_{a1} = \left(\frac{\Delta x}{2\theta\,\Delta t} - 2I_e\right)\frac{1}{A_u}$$

$$M_{a2} = -\frac{g}{B_u} - \frac{Q_u}{A_u}\left(M_{a1} + \frac{g\,S_{eu}\,w_u\,\Delta x}{Q_u}\right)$$

$$M_{a3} = \left(\frac{\Delta x}{2\theta\,\Delta t} + 2J_e\right)\frac{1}{A_d}$$

$$M_{a4} = \frac{g}{B_d} - \frac{Q_d}{A_d}\left(M_{a3} + \frac{g\,S_{ed}\,w_d\,\Delta x}{Q_d}\right)$$

$$M_{a5} = \frac{1}{\theta}\left[I_e\frac{Q_u}{A_u} - J_e\frac{Q_d}{A_d} + g(h_u - h_d)\right]$$

An efficient strategy for computing the solution (inverse) matrix is to reduce Equations (14) and (15) into triple diagonal form by analytical elimination, first of one of the downstream variables, then of one of the upstream variables. The rapid tri-diagonal algorithm can then be applied directly – see Cunge *et al.* (1980).

This solves for the variations, which can then be added to the values at the previous time step to provide the new solution.

COMPARATIVE TESTING

Steady flow

Note that in steady flow, the right hand sides of Equations (14) and (15) will both be zero, so with steady boundary conditions the variations will, in time, all diminish to zero. The solution will then be steady and coincide exactly (within the limitations of round-off error) with a solution obtained by steady flow analysis. Other unsteady flow solutions are sometimes described as converging to a 'quasi-steady' flow, but if this differs from exact steady flow, then the solution must be faulty.

In steady-state problems, shocks may still occur as standing hydraulic jumps. Another computationally challenging area is the free overfall, where standard textbook analysis (e.g., Henderson 1966) indicates that the flow is critical and water surface slope becomes infinite. Robust solutions need to be able to cope with such singularities, and here the analysis of shock fronts by Whitham (1955) is useful.

In Barnett (2012) comparison was made between CELL Integrals and the finite difference method with two fixed weightings: Upstream Differencing and Central Differencing. The CELL Integral solution was that implemented in the *AULOS* package (HYDRA 2013). The three schemes were first compared using tests C1 and C2 published by the UK DEFRA/Environmental Agency (2004).

Because the test conditions were not far from uniform flow, only minor comparative differences were seen, but the C2 test featured enough of a drawdown profile to show that the Central Difference scheme was less robust than either the Upstream Difference or CELL Integral scheme.

A more severe test was then applied, drawing the flow down to critical flow at the downstream end, and producing a more significant deterioration of the Central Difference solution with coarse grids. In addition, the CELL Integral scheme proved to outperform the Upstream Difference scheme, which required 500 m grid spacing to match the Cell Integral solution at 1,000 m grid spacing.

Backwater curve analysis from a previous paper (Barnett & MacMurray 1998) was then replotted on the same basis as the drawdown curves. In this case, the Upstream Difference solution was clearly less robust than the Central Difference or CELL Integral solution, requiring grid spacing refinement to 100 m to match the other two at 500 m grid spacing. At very coarse (1,000 m) grid spacing, only the CELL Integral scheme continued to match the convergent solution upstream of the test reach.

Unsteady flow case study: Dambreak wave

A widely quoted standard (e.g., Sanders 2001; Barnett 2003) dambreak test is that undertaken by the Waterways Experiment Station (1960). This requires the model to deal both with the positive wave downstream after the dambreak, and with the negative wave through the reservoir upstream. The experimental results are of accuracy constrained by the limitations of instrumentation available at the time, but the scale of the experiment was in the fully turbulent range of Reynolds Number, unlike some more recent cases.

The particular test of interest is WES Test 5.1, in which the breach was a rectangular shape at full depth, but only extending 1/10 of the channel width. The edges of the breach were not described directly in the study report, but appear from photographs to be sharp-edged. Accordingly, a width contraction discharge coefficient of 0.9 was applied to the aperture as recommended by Henderson (1966). To support the treatment of the aperture as a structure, it was modelled using an energy balance CELL, while the remainder of the channel was treated using momentum balance CELLs to represent shocks as Whitham fronts.

While the model could be run from dry downstream conditions, it has proved to be very difficult to provide a robust solution for the wetting front, as the Courant Number of the wave front simulation cannot then greatly exceed unity. This problem was addressed by Mynett (1999), who described algorithmic methods of ensuring that the water depth was always positive throughout the solution.

Alternatively, initiating the solution with minimal flows at all computation points has been found to allow fully implicit solutions with front Courant Numbers orders of magnitude larger for robust model computation. This considerable benefit is achieved without affecting calibration at high resolution. Therefore the effect of the sudden opening was simulated by drawing the model down from a static start to the specified reservoir level with the aperture set at a height to provide a small flow (approximately 1 litre/s, or 3% of maximum flows) to be maintained downstream. For the same reason, a small invert slot was provided to prevent upstream drying as the reservoir emptied.

At the moment of dambreak, the solution was hot started from the drawdown solution, but with the full sharp-edged aperture open. The model therefore responded to this change over a time scale of one time step, compared with the experimental removal time quoted as 0.01–0.03 s. The accepted value of Manning $n = 0.009$ was applied and the dimensions were otherwise as given in the literature.

'Fine' calibration

To begin, convergence was sought at high resolution to provide a benchmark for robustness tests. Figure 2 shows in heavy lines the adopted 'fine' solution which used $\Delta x = 0.2$ m, $\Delta t = 0.4$ s, and compares this with the experimental data.

The dotted lines show the closely similar solutions for $\Delta x = 0.2$ m, $\Delta t = 0.3$ s, establishing that convergence is essentially complete. The calibration shows a good fit for water levels, especially at the front location and at peak flows. The recession curve has experimental data a little more scattered, but it must be borne in mind that level values were read only to the nearest 0.01 feet (about 3 mm).

This calibrated 'fine' solution is then added to the two subsequent plots (Figures 3 and 4) to provide a basis for evaluation of solution robustness. Note that the front celerity was measured as reducing from 0.85 m/s near the breach to about 0.7 m/s further downstream, so the front Courant Number is around unity for the time step of 0.3 s, and attempts to reduce the time step further were unsuccessful.

This suggests that the usual claimed unconditional stability for implicit solutions applies only down to Courant Numbers of unity, consistent with the analysis (Barnett 1974) which suggests boundary condition variations tend to destabilise implicit solutions below this mark.

Solution robustness with a fine spatial grid

Figure 3 compares solutions with a spatial grid of $\Delta x = 0.2$ m, testing values of $\Delta t = 4$, 10 and 60 s in comparison with the original 'fine' solution using $\Delta t = 0.4$ s.

All of the solutions ran to completion, even that with a front Courant Number of about 200, so the CELL Integral solution meets the minimum robustness requirement of not failing using time steps varying by two orders of magnitude.

The solutions with longer time steps all show overshoot of flow in the wave front, probably caused by coarse

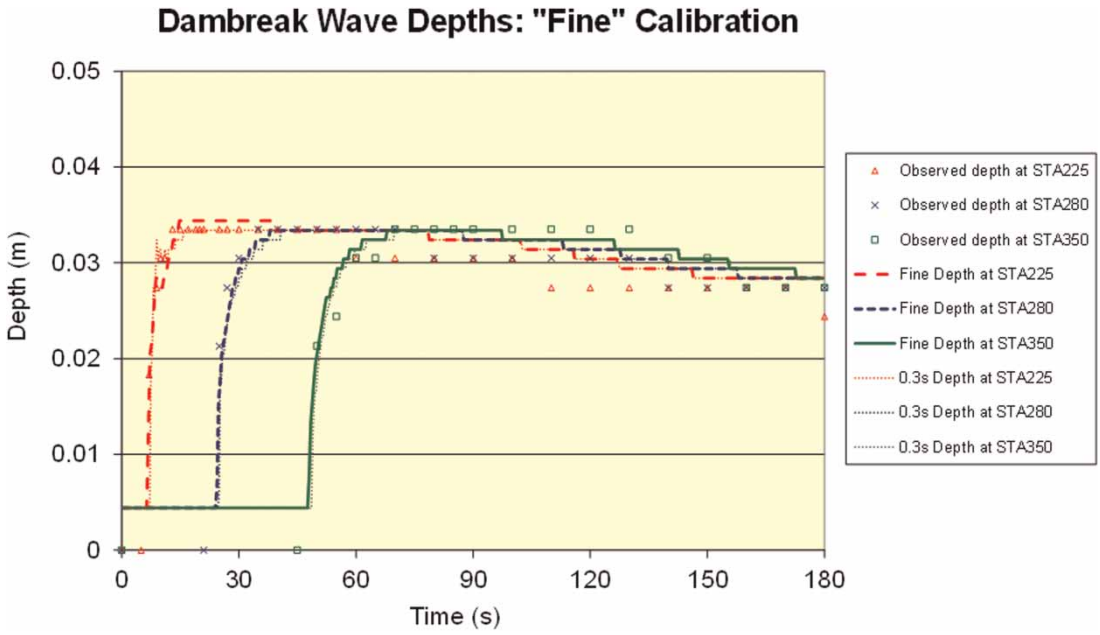

Figure 2 | 'Fine' calibration.

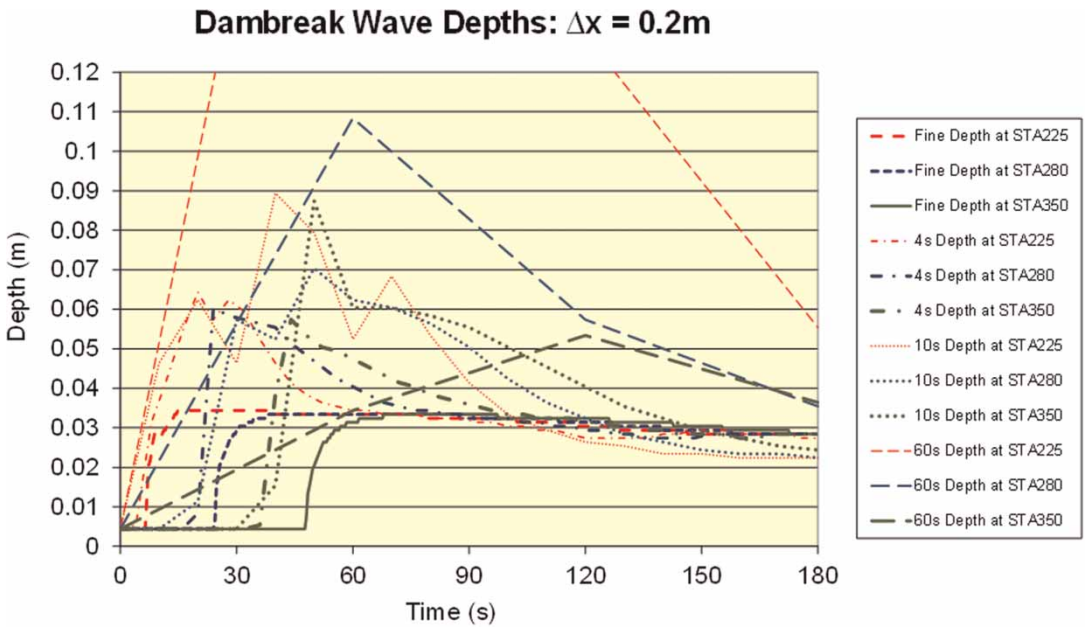

Figure 3 | Solutions at fine spatial grids.

resolution of the dam breach outflow corresponding with the initial step change in level being effective throughout the period defined by the first time step. The solution with a time step of 4 s (chain dotted lines) shows some initial overshoot, this gets worse with the 10 s solution (dotted lines), while the 60 s solution (long dashed lines) grossly overshoots, but still in a stable manner. The shock wave speed shows a phase advance, particularly in the 4 s

solution, but considering the extreme limitations of the timewise resolution this phase error does not seem to increase thereafter.

Solution robustness with a coarse spatial grid

Figure 4 shows the results using a spatial grid of $\Delta x = 2$ m, again testing values of $\Delta t = 4$, 10 and 60 s. The original 'fine' solution using $\Delta x = 0.2$ m is retained for comparison.

Again, all solutions passed the minimum robustness requirement of not failing. For the 4 s solution, the shock Courant Number is now the same as for the 'fine' solution, and this produces an excellent correspondence in shock wave speeds. However, there is still a stable overshoot, presumably again caused by the coarse timewise resolution of the dam breach outflow.

The maximum shock Courant Number only reaches about 20 this time, and the resulting solutions appear to settle to a reasonable approximation of the 'fine', bearing in mind the limitations of the timewise resolution.

Discussion

The dambreak solutions have proved to be robust, reliably providing a coarse approximation to the 'fine' solution even for Courant Numbers and spatial grids varying by orders of magnitude. This robustness property has great importance, as sudden variations in flow may occur in unexpected places in solutions of large networks in practical model applications. It is not helpful if the solution simply collapses in such cases, as this obliges the model user to divert considerable time to fault diagnosis, in which the problem area may not be apparent. With robust solutions, the location of a possible problem is obvious, and because the computation is not terminated by solution failure the model user is free to elect to accept the coarse solution.

If the modelling exercise was focused on the single event shown in the selected channel, the coarsest solutions in Figures 3 and 4 would of course be rejected, as a simple test of halving the time step would quickly establish that convergence was still some way off. This would also be expected by violation in the coarser time steps of the assumptions

$$\frac{\dot{Q}}{Q} \ll 1 \quad \frac{\dot{A}}{A} \ll 1$$

used to linearise the likes of Equation (13).

Further, the fine grid solutions are strongly concave upwards during wave initiation as shown in Figure 4. Describing the beginning-to-peak inflow by drawing a

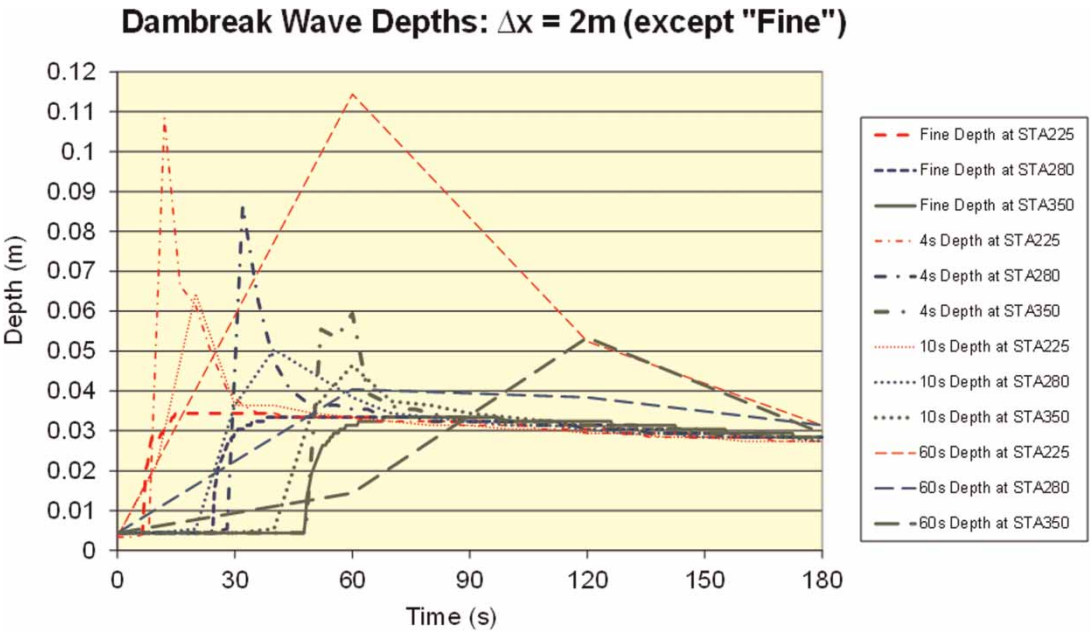

Figure 4 | Solutions at coarse spatial grids.

straight line from $t = 0$ to $t = 60$ (as is required using linear interpolation over 60 s time steps) will greatly overestimate the flow volume entering upstream and hence the estimate of depth after one time step.

However, if this event occurred during a long-term simulation of duration, say 50 years, then even the coarse results would be quite adequate for screening purposes, as the main aim would then be detection and ranking of severe events against a background of lengthy spells of low flow. Similarly, if the channel was a small part of an extensive drainage network, the success of the overall simulation would depend more on completion of the solution than on high accuracy in a minor link.

CONCLUSIONS

Applied modelling projects typically deal with extensive networks in which a wide distribution of flow hydrographs pass along the various channels. In these conditions, spatial grids can rarely be designed anticipating uniformity of Courant Numbers in all parts of the model, even within one order of magnitude. Robustness of a model solution is therefore fundamental to solution reliability, and tolerance of a considerable range of conditions is required in practice if much project time is not to be wasted on fault diagnosis and correction.

Finite integral analysis is drawn from informal practice in classical hydraulics, and CELL Integral methods lead to a new set of fundamental balance equations, the Full Hydraulic equations. These are a superset of other classical systems of equations, such as the Navier–Stokes or St Venant equations, which are limited by the exclusion of energy analysis through structures and by the restriction (invalid in hyperbolic problems) that all variables must be continuous. These restrictions can be avoided by the use of convergent power series to linearise the integral expressions, as demonstrated for streamtube hydraulics by the successful derivation of a full matrix of coefficients for computational solution of each of mass, momentum and energy balances.

For steady flow, the results of two industry standard benchmarking tests defined by the UK DEFRA/Environment Agency have been published. In addition, studies of a backwater curve and a drawdown to critical flow have been referenced. These tests were run with successively finer grid discretisation over three orders of magnitude, and the convergence of the CELL Integral results was compared with finite difference methods using conventional Upstream Differencing and Central Differencing. Central Differencing is more robust than Upstream Differencing in backwater curves. The reverse applies for drawdown curves, as the Central Differencing solution diverges rapidly above a certain step size threshold. However, the CELL Integral schemes (as implemented in the *AULOS* package) were found to be significantly more robust than both of the finite difference schemes, converging to the common fine grid solution at steps up to an order of magnitude larger.

In unsteady flow, a standard dambreak case study was tested over progressively coarser grids covering two orders of magnitude in Courant Numbers, demonstrating an ability to accommodate severe shocks even in solutions with minimal resolution. With simple post-computation inspection procedures sufficient to prevent unacceptable loss of accuracy, this offers users of CELL Integral solutions greatly increased computational speed and grid flexibility.

REFERENCES

Abbott, M. B. 1979 *Computational Hydraulics*. Pitman, London.

Barnett, A. G. 1974 On the Stability of Centred Implicit Difference Schemes. *Proc. Fifth Australasian Conference on Hydraulics and Fluid Mechanics*, Christchurch II, 537–543.

Barnett, A. G. 1994 On the Basis of Hydraulic Computation. *Proc. 1st International Conference on Hydroinformatics*, Delft, 1, 127–132.

Barnett, A. G. 1995 Modelling of inundation management in extreme storms. *Water Sci. Tech*. **32** (1), 201–207.

Barnett, A. G. 2003 Discussion of Sanders B.F. High-resolution and non-oscillatory solution of the St. Venant equations in non-rectangular and non-prismatic channels. *J. Hyd. Res* **41** (6), 668–672.

Barnett, A. G. 2012 Comparison of solution robustness and convergence on coarse grid models. *Proc. HIC 2012*, Hamburg, Paper 120.

Barnett, A. G. & MacMurray, H. L. 1998 Two comparisons of CELL Integral and finite difference solutions. *Proc. Hydroinformatics 1998*, Copenhagen, 1, 17–24.

Batchelor, G. K. 1970 *An Introduction to Fluid Dynamics*. Cambridge University Press, Cambridge, UK.

Cunge, J. A., Holly, F. M. & Verwey, A. 1980 *Practical Aspects of Computational River Hydraulics*. Pitman, London.

DEFRA/Environment Agency 2004 Benchmarking Hydraulic River Modelling Software Packages Results – Test C (Triangular Channels). Technical Report W5-105/TR2C.

Garcia-Navarro, P. & Brufau, P. 2006 Numerical methods for the shallow water equations: 2D approach. In: *River Basin Modelling for Flood Risk Mitigation* (D. W. Knight & A. Y. Shamseldin, eds). Taylor & Francis, London, pp. 409–428.

Garcia-Navarro, P. & Burguete, J. 2006 Numerical methods for the shallow water equations: 1D approach. In: *River Basin Modelling for Flood Risk Mitigation* (D. W. Knight & A. Y. Shamseldin, eds). Taylor & Francis, London, pp. 387–408.

Guinot, V. 2000 Linear advection modelling: The issue of divergent flows. *J. Hydroinform*. **2**, 113–121.

Henderson, F. M. 1966 *Open Channel Flow*. Macmillan, New York.

HYDRA Software Ltd 2013 Available at: www.auloshydraulics.com.

Landau, L. D. & Lifshitz, E. M. 1959 *Fluid Mechanics*. Pergamon, London.

Landau, L. D. & Lifshitz, E. M. 1972 *Mechanics and Electrodynamics*. Pergamon, London.

Milne-Thomson, L. M. 1972 *Theoretical Hydrodynamics*. Macmillan, London.

Mynett, A. E. 1999 Hydroinformatics and its applications at Delft Hydraulics. *J. Hydroinform*. **1**, 83–102.

Norris, S. E., Were, C. J., Richards, P. J. & Mallinson, G. D. 2011 A Voronoi-based ALE solver for the calculation of incompressible flow on deforming unstructured meshes. *Int. J. Numer. Method Fluids* **65**, 1160–1179.

Samuels, P. G. 2006 Risk and uncertainty in flood management. In: *River Basin Modelling for Flood Risk Mitigation* (D. W. Knight & A. Y. Shamseldin, eds). Taylor & Francis, London, pp. 481–517.

Sanders, B. F. 2001 High resolution and non-oscillatory solution of the St. Venant equations in non-rectilinear and non-prismatic channels. *J. Hyd. Res*. **39**, 321–330.

Waterways Experiment Station 1960 Floods Resulting from Suddenly Breached Dams, Miscellaneous Paper No. 2-374, US Army Corps of Engineers, Report 1, Conditions of Minimum Resistance, Vicksburg, MS.

W3C Working Draft 2012 Available at: www.w3.org/Math/characters/html/symbol.html.

Whitham, G. B. 1955 The effects of hydraulic resistance on the dam-break problem. *Proc. Royal Society A* **227** (1170), 399–407.

First received 19 April 2013; accepted in revised form 13 August 2013. Available online 19 September 2013